Hindrance of the excitation of the Hoyle state and the ghost of the 2_2^+ state in ^{12}C

Dao T. Khoa[1], Do Cong Cuong[1], Yoshiko Kanada-En'yo [2]

[1]*Institute for Nuclear Science & Technique, VAEC*
179 Hoang Quoc Viet Rd., Nghia Do, Hanoi, Vietnam.
[2] *Department of Physics, Kyoto University, Kyoto 606-8502, Japan.*

Abstract

While the Hoyle state (the isoscalar 0_2^+ excitation at 7.65 MeV in ^{12}C) has been observed in almost all the electron and α inelastic scattering experiments, the second 2^+ excited state of ^{12}C at $E_\mathrm{x} \approx 10$ MeV, believed to be an excitation of the Hoyle state, has not been clearly observed in these measurements excepting the high-precision $(\alpha, \alpha')^{12}$C experiments at $E_\alpha = 240$ and 386 MeV. Given the (spin and isospin zero) α-particle as a good probe for the nuclear isoscalar excitations, it remains a puzzle why the peak of the 2_2^+ state could not be clearly identified in the measured $(\alpha, \alpha')^{12}$C spectra. To investigate this effect, we have performed a microscopic folding model analysis of the $\alpha + {}^{12}$C scattering data at 240 and 386 MeV in both the Distorted Wave Born Approximation (DWBA) and coupled-channel (CC) formalism, using the nuclear transition densities given by the antisymmetrized molecular dynamics (AMD) approach and a complex CDM3Y6 density dependent interaction. Although AMD predicts a very weak transition strength for the direct $(0_1^+ \to 2_2^+)$ excitation, our detailed analysis has shown evidence that a weak *ghost* of the 2_2^+ state could be identified in the 240 MeV $(\alpha, \alpha')^{12}$C data

for the 0_3^+ state at 10.3 MeV, when the CC effects by the indirect excitation of the 2_2^+ state are taken into account. Based on the same AMD structure input and preliminary $(\alpha, \alpha')^{12}$C data at 386 MeV, we have estimated relative contributions from the 2_2^+ and 0_3^+ states to the excitation of ^{12}C at $E_\mathrm{x} \approx 10$ MeV as well as possible contamination by 3_1^- state.

The excited states of ^{12}C lying around the α-decay threshold have become a research subject of wide interest recently [1, 2] because of the dominant α-cluster structure established in some cases, such as the isoscalar 0_2^+ state at 7.65 MeV in ^{12}C (known as the Hoyle state that has a vital role in the stellar synthesis of Carbon). Although the three α-cluster structure of the Hoyle state has been shown more than 30 years ago in the microscopic Resonating Group Method (RGM) calculations [3, 4, 5], an interesting α-condensate scenario [2] for this state has been established just recently [6, 7], where three α clusters were shown to condense into the lowest S state of their potential. A more complicated structure of the Hoyle state was found in the Fermionic Molecular Dynamics (FMD) calculation [8] where the condensate wave function is mixed also with the molecular ^{8}Be$+\alpha$ configuration, but the condensate component still exhausts about 70% of the total wave function. Given such a strong condensate of the three α clusters, a question arises naturally about the isoscalar (IS) excitation of the Hoyle state. Namely, if it is a condensate S state then the next level in the potential containing three α-particles should be a D state formed by promoting an α-particle from the S to D level. Such an excited state has been first predicted by

2

Funaki *el al.* [9] and it must be a 2^+ state at the excitation energy of around 10 MeV, with a pronounced $^8\text{Be}+\alpha$ structure [1]. This same 2_2^+ state has been predicted also by the three-body calculation [10] or the antisymmetrized molecular dynamics (AMD) approach [11], as the second 2^+ state of ^{12}C lying about 2 MeV above the α-decay threshold. The experimental observation of the 2_2^+ state of ^{12}C would be very important for a deeper understanding of the Hoyle state, e.g., the measured excitation energy would allow us to determine the moment of inertia and deformation of ^{12}C being in the Hoyle state. The first experimental hint for the 2_2^+ state has been found by the Texas A&M University group in the isoscalar $E2$ strength distribution of ^{12}C in the energy range $10 \lesssim E_\text{x} \lesssim 30$ MeV [12]. However, this 2^+ peak is located at $E_\text{x} \approx 11.46\pm0.20$ MeV which is somewhat high compared to the predicted value around 10 MeV. A more convincing experimental measurement of the 2_2^+ state has been performed by Itoh *et al.* in the 386 MeV inelastic $\alpha+^{12}\text{C}$ scattering spectrum [13, 14], based on a multipole decomposition analysis (MDA) of the measured $(\alpha, \alpha')^{12}\text{C}$ angular distribution. Given a prominent 3-α cluster structure predicted for this state, several experimental efforts [15, 16] have also been made by Freer *et al.* to search for the 2_2^+ peak in the 3-α decay spectrum of ^{12}C in the excitation energy range of $9 \lesssim E_\text{x} \lesssim$ 11 MeV but no positive identification has been done. Recently, Freer and collaborators have performed the $(p, p')^{12}\text{C}$ experiment at the beam energy of 66 MeV [17] as well as the $(^{12}\text{C},^{12}\text{C}^*)^{12}\text{C}$ experiment at 101.5 MeV [18]. While some enhancement above background has been deduced from the $(p, p')^{12}\text{C}$ spectrum that indicates a possible 2_2^+ peak at 9.6 ± 0.1 MeV [17], no conclusive evidence was found in the latter experiment excepting some estimate made

3

for the upper limits in the excitation strength of the 2_2^+ state [18]. The present work is our attempt to shed some light into this puzzled situation by a detailed folding model analysis of inelastic $\alpha+^{12}C$ scattering data at 240 MeV [12] and 386 MeV [13, 14].

Because the spin- and isospin zero α-particle is a very good projectile to excite the nuclear IS states, the 3-α RGM wave function obtained by Kamimura [4] has been used earlier in the folding model analysis [19] of the inelastic $\alpha+^{12}C$ scattering to probe the $E0$ transition strength of the Hoyle state. This approach has been extended to study also other IS excitations of ^{12}C like 2^+ (4.44 MeV), 3^- (9.64 MeV), 0^+ (10.3 MeV) and 1^- (10.84 MeV) states [20], using the same RGM wave functions. The technical details of this folding approach for elastic and inelastic nucleus-nucleus scattering can be found in Ref. [21]. The key quantity in our folding model analysis is the α-nucleus form factor (FF) that contains all the information about the α-nucleus inelastic scattering as well as structure of the nuclear state under study. Therefore, it is vital to evaluate the FF using a good choice for the effective nucleon-nucleon (NN) interaction and realistic wave functions for the α-particle and target nucleus, respectively. In the present work, we apply our folding model approach to study the possible excitation of the 2_2^+ state of ^{12}C using the microscopic nuclear transition densities given by the AMD calculation [11] and the (complex) density-dependent CDM3Y6 interaction, whose parameters have been fine tuned recently [22] for the α-nucleus scattering at the same incident energies of 240 and 386 MeV.

The AMD approach has been proven to be quite reliable in describing the structure of low-lying excited states in light nuclei, where both the clus-

ter and shell-model like states are consistently reproduced [11, 23]. In the present work, the structure of IS excited states of ^{12}C is generated within the AMD approach using the method of variation after the spin-parity projection (VAP). The main structure properties of these states are summarized in Table 1. While the AMD prediction for the shell-model like 2_1^+ state is quite satisfactory in both the excitation energy and $E2$ transition strength, the predicted excitation energies for higher lying states are slightly larger than the experimental values. However, such a difference in the excitation energies does not affect significantly the calculated inelastic $\alpha+^{12}$C scattering cross section because it can lead only to a very small change in the kinetic energy of emitted α-particle and, thus, can be neglected. Most vital are the strength and shape of the nuclear transition density used to evaluate the inelastic FF that can affect directly the inelastic scattering cross section calculated in the Distorted Wave Born Approximation (DWBA) or coupled-channel (CC) formalism. The details of the AMD calculation for the IS excited states of ^{12}C are given in Ref. [11]. In the present work, the AMD nuclear transition densities enter the folding calculation in the same convention as in Refs. [21, 22] so that the isoscalar transition strength for a 2^λ-pole nuclear transition $|J_i\rangle \rightarrow |J_f\rangle$ is described by the reduced nuclear transition rate $B(\mathrm{IS}\lambda; J_i \rightarrow J_f) = |M(\mathrm{IS}\lambda; J_i \rightarrow J_f)|^2$, where the 2^λ-pole transition moment is determined from the corresponding nuclear transition density as

$$M(\mathrm{IS}\lambda; J_i \rightarrow J_f) \;=\; \int dr \; r^{\lambda+2} \rho_{J_f,J_i}^{(\lambda)}(r) \quad \text{if} \quad \lambda \geqslant 2, \tag{1}$$

$$M(\mathrm{IS}0; J_i \rightarrow J_f) \;=\; \int dr \; r^4 \rho_{J_f,J_i}^{(\lambda=0)}(r), \tag{2}$$

$$M(\mathrm{IS}1; J_i \rightarrow J_f) \;=\; \int dr \left(r^3 - \frac{5}{3}\langle r^2\rangle r \right) r^2 \rho_{J_f,J_i}^{(\lambda=1)}(r). \tag{3}$$

Note that the IS dipole transition moment is evaluated based on higher-order corrections to the dipole operator, with spurious center-of-mass (c.m.) oscillation subtracted [24]. The reduced electric transition rate is evaluated as $B(E\lambda; J_i \to J_f) = |M(E\lambda; J_i \to J_f)|^2$, where $M(E\lambda)$ is determined in the same way as $M(\text{IS}\lambda)$ but using the proton part of the nuclear transition density only. We will discuss hereafter the transition strength in terms of $B(E\lambda)$ only because this is the quantity that can be compared with the experimental data whenever possible.

The excitation energies and $E\lambda$ transition strengths of the IS states considered in the present work are given in Table 1. One can see that the calculated excitation energies and $E\lambda$ transitions from the ground state 0_1^+ to the 2_1^+, 0_2^+ and 3_1^- states agree reasonably with the experimental values. As illustrated in Figs. 1 and 2 below, the AMD nuclear transition densities also give good description of the corresponding inelastic $(\alpha, \alpha')^{12}\text{C}$ cross sections. In difference from the shell-model like structure of the 2_1^+ state, the 2_2^+ state has a well established cluster structure (see Fig. 5 of Ref. [11]), with a more extended and dilute mass distribution that corresponds to the mass radius $R_\text{m} \approx 3.99$ fm which is even larger than that of the Hoyle state. The more striking are the predicted electric transition rates for the $E2$ transitions from the Hoyle state to the 2_2^+ state and from the 2_2^+ state to the 4_2^+ state: $B(E2; 0_2^+ \to 2_2^+) \approx 511 \ e^2\text{fm}^4$ and $B(E2; 2_2^+ \to 4_2^+) \approx 1071 \ e^2\text{fm}^4$ that are much stronger than those of the $E2$ transitions between the members of the ground-state rotational band: $B(E2; 0_1^+ \to 2_1^+) \approx 42.5 \ e^2\text{fm}^4$ and $B(E2; 2_1^+ \to 4_1^+) \approx 28.5 \ e^2\text{fm}^4$. As a result, the predicted $B(E2; 0_2^+ \to 2_2^+)$ and $B(E2; 2_2^+ \to 4_2^+)$ transition rates strongly suggest that the 2_2^+ and 4_2^+

6

states should be the members of the excited rotational band built upon the Hoyle state. The $B(E2; 0_2^+ \to 2_2^+)$ values predicted by the RGM [4] and FMD calculations [25] are even larger than that given by the AMD calculation. Given a very weak direct excitation of the 2_2^+ state from the ground state, $B(E2; 0_1^+ \to 2_2^+) \approx 2 \ e^2\mathrm{fm}^4$ predicted by the AMD calculation, we can draw a conclusion that the 2_2^+ state should be an IS quadrupole excitation of the Hoyle state [1]. It should be noted that if we take the measured $E2$ strength of the 2_2^+ peak at 11.46 MeV in the 240 MeV $(\alpha, \alpha')^{12}\mathrm{C}$ spectrum, which exhausts $2.15 \pm 0.30\%$ of the $E2$ energy weighted sum rule (EWSR) [12], then we obtain $B(E2; 0_1^+ \to 2_2^+)_\mathrm{exp} \approx 2.5 \pm 0.5 \ e^2\mathrm{fm}^4$ based on the standard collective model treatment of the MDA [22]. This value agrees surprisingly well with that predicted by the AMD calculation and it is, therefore, not excluded that the observed 2^+ peak at $E_\mathrm{x} \approx 11.46$ MeV in the 240 MeV $(\alpha, \alpha')^{12}\mathrm{C}$ spectrum corresponds to the 2_2^+ state, although the excitation energy is about 1 MeV above the value predicted by the AMD. The width of this state has been determined from the 240 MeV spectrum to be $\Gamma_\mathrm{c.m.} \approx 430 \pm 100$ keV [12], which is somewhat smaller than that (~ 600 keV) suggested by Freer *et al.* [17]. A closer look indicates that the 2^+ peak at 11.46 MeV in the 240 MeV spectrum might well be the adopted (2^+) level of $^{12}\mathrm{C}$ [26] at $E_\mathrm{x} \approx 11.16 \pm 0.05$ MeV having a width of 550 ± 100 keV, observed in the $(^3\mathrm{He},d)$ stripping reaction at $E_\mathrm{lab} = 44$ MeV [27]. It should be noted, however, that this state has only been seen once in the $^{11}\mathrm{B}(^3\mathrm{He},d)$ reaction, and not in other studies. Therefore, it is not excluded that this observation was actually a target contaminant, which it was not possible to establish in the measurements due to limitations in the focal plane detector. We note

7

further that the 2_2^+ and 0_3^+ states have been shown by the FMD calculation [25] to be nearly degenerate at the excitation energy $E_x \approx 11.8 \sim 11.9$ MeV. Consequently, the probability is high that the 2_2^+ state is indeed the peak observed at $E_x \approx 11.46$ MeV in the 240 MeV $(\alpha, \alpha')^{12}$C spectrum [12].

To further investigate the excitation of the 2_2^+ state in the $(\alpha, \alpha')^{12}$C experiment, we have used the AMD nuclear transition densities in our folding model analysis of inelastic $\alpha + ^{12}$C scattering data measured with high precision at $E_\alpha = 240$ MeV [12] and 386 MeV [13, 14]. A generalized double-folding method [21] was used to calculate the complex $\alpha + ^{12}$C potential as the following Hartree-Fock-type matrix element of the complex CDM3Y6 interaction [22, 32].

$$U_{A \to A^*} = \sum_{i \in \alpha; j \in A, j' \in A^*} [\langle ij'|v_D|ij \rangle + \langle ij'|v_{EX}|ji \rangle], \tag{4}$$

where A and A^* are states of ^{12}C target in the entrance- and exit channels of the $\alpha + ^{12}$C scattering, respectively. Thus, Eq. (4) gives the (diagonal) elastic optical potential (OP) if $A^* = A$ and inelastic scattering FF if otherwise. The complex density-dependent direct and exchange parts of the CDM3Y6 interaction $v_{D(EX)}$ were taken the same as those parametrized recently [22] for the study of $\alpha + ^{208}$Pb scattering at 240 and 386 MeV. The accurate local density approximation suggested in Refs. [22, 33] has been used for the exchange term in Eq. (4). All the DWBA and CC calculations have been performed using the CC code ECIS97 written by Raynal [34]. The real and imaginary elastic folded potential were scaled by the coefficients N_R and N_I, respectively, for the best optical model (OM) fit of the elastic scattering data: $N_R \approx 1.1, N_I \approx 1.4$ and $N_R \approx 1.3, N_I \approx 1.6$ for $E_\alpha = 240$ and 386

Table 1: Excitation energies and $E\lambda$ transition strengths of the IS states of ^{12}C under present study. Results of the AMD calculation [11] are compared with the available experimental data. Note that $M(E\lambda)$ is given in e fm$^{\lambda+2}$ for 0^+ and 1^- states; the experimental $B(E2; 2^+_2 \to 0^+_1)$ value has been deduced from the $E2$ EWSR strength given in Ref. [12] for the 2^+ peak observed at $E_x \approx 11.46$ MeV.

J^π	E_{calc} (MeV)	E_{exp} (MeV)	Transitions	Calc. (e^{2}fm$^{2\lambda}$)	Exp. (e^{2}fm$^{2\lambda}$)	Ref.
2^+_1	4.5	4.44	$B(E2; 2^+_1 \to 0^+_1)$	8.5	8.0 ± 0.8	[28]
			$B(E2; 2^+_1 \to 4^+_1)$	28.5		
0^+_2	8.1	7.65	$M(E0; 0^+_2 \to 0^+_1)$	6.7	5.4 ± 0.2	[29]
			$B(E2; 0^+_2 \to 2^+_1)$	25.5	13.0 ± 2.0	[30]
			$B(E2; 0^+_2 \to 2^+_2)$	511		
3^-_1	10.8	9.64	$B(E3; 3^-_1 \to 0^+_1)$	106	87.1 ± 1.3	[31]
			$B(E3; 3^-_1 \to 2^+_2)$	137		
0^+_3	10.7	10.3	$M(E0; 0^+_3 \to 0^+_1)$	2.3		
			$B(E2; 0^+_3 \to 2^+_2)$	1553		
2^+_2	10.6	$9 \sim 11.5$	$B(E2; 2^+_2 \to 0^+_1)$	0.4	0.5 ± 0.1	[12]
			$B(E2; 2^+_2 \to 0^+_2)$	102		
			$B(E2; 2^+_2 \to 4^+_1)$	13.5		
			$B(E2; 2^+_2 \to 4^+_2)$	1071		
1^-_1	12.6	10.84	$B(E3; 1^-_1 \to 2^+_2)$	1679		
			$M(E1; 1^-_1 \to 0^+_1)$	2.56		

MeV, respectively. These same $N_{\mathrm{R(I)}}$ factors were used to scale the real and imaginary inelastic folded FF for the DWBA calculation, a standard method used so far in the folding + DWBA analysis of inelastic α-nucleus scattering [12, 21, 36]. Since N_{R} and N_{I} are an approximate way to take into account the higher-order (dynamic polarization) contributions to the microscopic OP [21], they must be readjusted again in the CC calculation to account for those nonelastic channels that were not included into the CC scheme. We then obtained $N_{\mathrm{R}} \approx 1.1, N_{\mathrm{I}} \approx 1.2$ and $N_{\mathrm{R}} \approx 1.2, N_{\mathrm{I}} \approx 1.3$ from the CC calculations for $E_\alpha = 240$ and 386 MeV, respectively. These $N_{\mathrm{R(I)}}$ factors were also used to scale the complex inelastic folded FF used in the CC calculation. The OM and CC descriptions of the elastic $\alpha + {}^{12}$C scattering at 240 MeV are shown in upper panel of Fig. 1. Our OM calculation not only well describes the elastic data but also gives the total reaction cross sections σ_{R} very close to the experimental values measured at the nearby energies. Thus, the (complex) double-folded OP should be accurate enough for the DWBA or CC analysis of inelastic $\alpha + {}^{12}$C scattering. For the 2^+_1 state, the electric transition rate predicted by the AMD, $B(E2, 0^+_1 \to 2^+_1) \approx 42.5 \ e^2\mathrm{fm}^4$, agrees perfectly with the measured value of $40 \pm 4 \ e^2\mathrm{fm}^4$ [28], and the corresponding inelastic FF describes the measured $(\alpha, \alpha')^{12}$C cross section quite satisfactory in both the DWBA and CC calculations (see lower panel of Fig. 1). The calculated $(\alpha, \alpha')^{12}$C cross section for the 2^+_1 state slightly underestimates the data at large angles and this could well be due to a strong refractive effect that implies a weaker absorption in the considered inelastic $(\alpha, \alpha')^{12}$C channel [35]. While the 2^+_1 state has been observed in the spectra of all inelastic $(\alpha, \alpha')^{12}$C experiments, the situation with the 2^+_2 state remains quite uncertain. Given
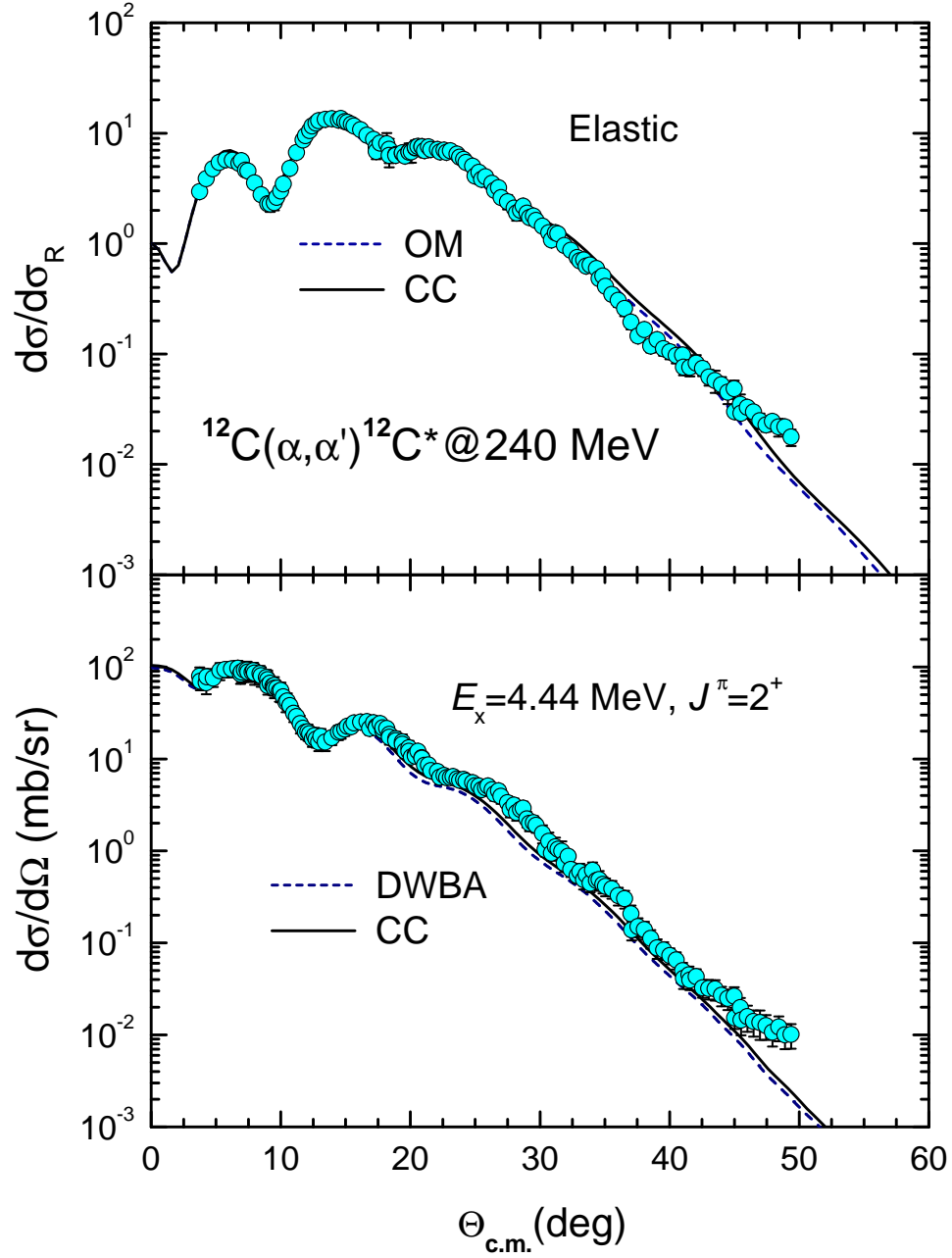
10

Figure 1: Elastic and inelastic $\alpha+{}^{12}C$ scattering data at $E_\alpha = 240$ MeV [12] measured for the 2^+_1 state at 4.44 MeV in comparison with the OM, DWBA and CC results given by the complex double-folded OP and inelastic FF.

the possible peak of the 2_2^+ state located at 9.6±0.1 MeV as deduced by Freer *et al.* from the $(p, p')^{12}$C spectrum [17], in the same location as the first 3^- state, it is highly suspected that the 2_2^+ peak could have been merged with the strong peak of the 3_1^- state and not observed in most of the measured $(\alpha, \alpha')^{12}$C spectra. In general, a 2^+ state should have angular distribution oscillating out-of-phase compared with that of the 3^- state and that effect could well be revealed in the $(\alpha, \alpha')^{12}$C angular distribution measured for the excitation energy $E_x \approx 9.6$ MeV if the 2^+ cross section is strong enough. To investigate this effect we have made the DWBA calculation of inelastic $\alpha + {}^{12}$C scattering at 240 MeV to the 3_1^- and 2_2^+ states and the calculated cross sections are compared with the data for the 3_1^- state in upper panel of Fig. 2. With the AMD transition density giving the electric transition rate $B(E3)$ rather close to the measured value (see Table 1), the inelastic FF based on the AMD transition density describes the measured $(\alpha, \alpha')^{12}$C cross section for the 3_1^- state quite well. Compared to the 3_1^- cross section, the predicted inelastic scattering cross section for the 2_2^+ state is much weaker, with the ratio of integrated $\alpha + {}^{12}$C cross sections $\sigma_{2_2^+}/\sigma_{3_1^-} \approx 12.8\%$. Such a strength ratio agrees reasonably with the upper limit of about 15% for the excitation strength of the 2_2^+ state versus that of the 3_1^- state deduced recently from the $({}^{12}$C, ^{12}C$^*)^{12}$C experiment at $E_{\text{lab}} = 101.5$ MeV [18]. Due to the *reversed* oscillating pattern, the 2_2^+ angular distribution is strongest versus the 3_1^- one at the most forward angles. At angles $\Theta_{\text{c.m.}} \gtrsim 10°$, the total $2_2^+ + 3_1^-$ cross section calculated in the DWBA nearly coincides with the 3_1^- cross section. The $(\alpha, \alpha')^{12}$C data points at forward angles also indicate strongly that the data are indeed deduced for the 3_1^- cross section and the contamination from
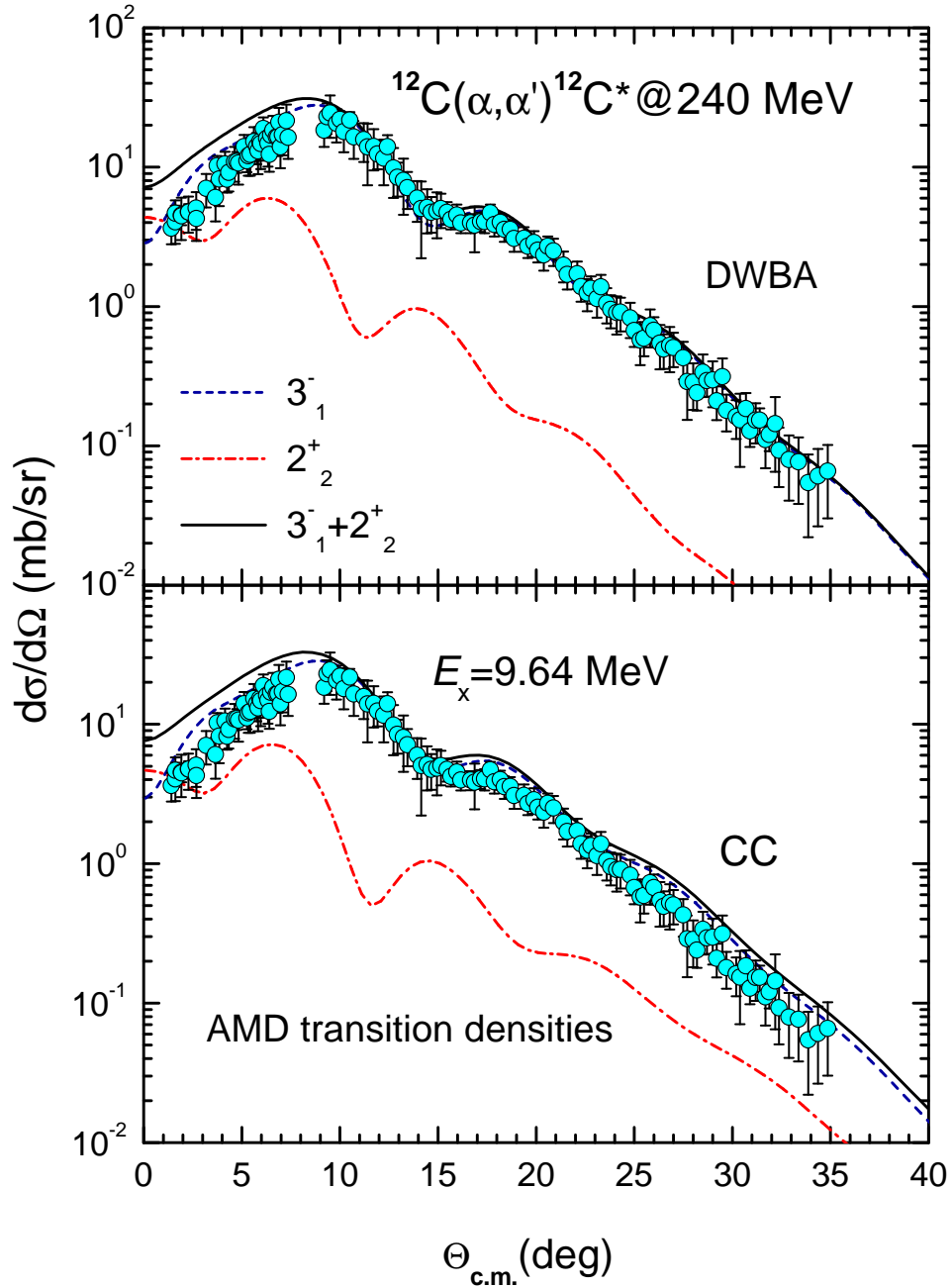
Figure 2: Inelastic $\alpha + {}^{12}$C scattering cross section measured for the 3_1^- state at 9.64 MeV [12] in comparison with the DWBA and CC results given by the complex double-folded inelastic FF based on the AMD nuclear transition densities for the 3_1^- and 2_2^+ states.
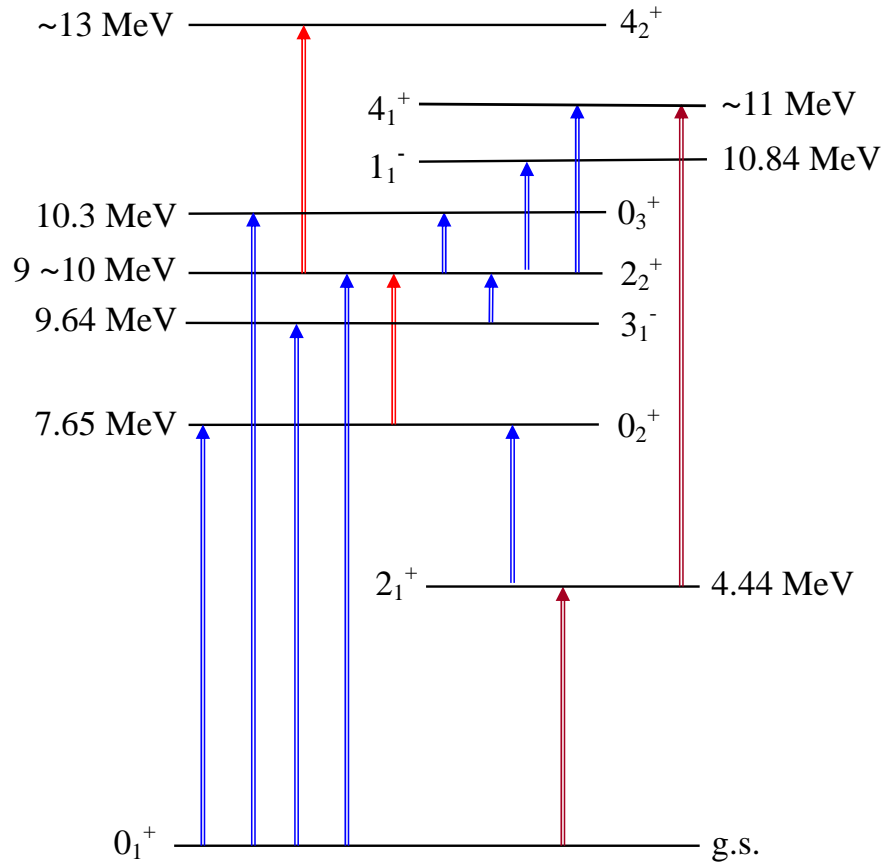
Figure 3: Coupling scheme used in the CC equations for the elastic and inelastic $\alpha+^{12}$C scattering.

the 2_2^+ state, if any, must be negligible. Therefore, in the case of 240 MeV data the excitation strength of the 2_2^+ state should be much smaller than 12.8% of the 3_1^- excitation strength if it is located at $E_x \approx 9.6$ MeV.

It should be recalled that DWBA only treats the direct excitation and one needs to perform the coupled-channel calculation in order to take into account contribution of the two-step excitation of the 2_2^+ state via the excited states of ^{12}C lying around $9 \sim 10$ MeV (see, e.g., very strong $E2$ transitions

from the Hoyle state or 0_3^+ state to the 2_2^+ state in Table 1). For this purpose, we have computed the AMD nuclear transition densities for all 13 transitions listed in Table 1 and obtained the corresponding inelastic scattering FF by the double-folding method (4) for the CC calculation. The coupling scheme is illustrated in Fig. 3 and the CC results for inelastic scattering to the 3_1^- state are shown in lower panel of Fig. 2. One can see that the contribution of the two-step excitation of the 2_2^+ state to the $(\alpha, \alpha')^{12}$C cross section is rather small but not negligible. It increases the 2_2^+ cross section by at least 10% and, hence, gives the ratio of integrated cross sections $\sigma_{2_2^+}/\sigma_{3_1^-} \approx 14.8\%$. Because the $E3$ transition linking the 3_1^- and 2_2^+ states is quite strong (see Table 1), the CC effect also enhances slightly the 3_1^- cross section. Nevertheless, it can be seen from Fig. 2 that the direct (one-step) $0_1^+ \to 2_2^+$ excitation of the 2_2^+ state is still dominant in the inelastic $\alpha+^{12}$C scattering at 240 MeV. Given a weak transition rate $B(E2, 0_1^+ \to 2_2^+) \approx 2~e^2\text{fm}^4$ predicted by the AMD, the 2_2^+ peak should be very difficult to disentangle from the $(\alpha, \alpha')^{12}$C spectrum if it stands just behind the strong 3_1^- peak. Moreover, the CC results and $(\alpha, \alpha')^{12}$C data points at forward angles (lower panel of Fig. 2) confirm consistently that the data points are indeed those for the 3_1^- state and the mixture of the 2_2^+ state should be negligible. In other words, the contribution of the 2_2^+ state to the inelastic $(\alpha, \alpha')^{12}$C cross section at $E_\text{x} \approx$ 9.6 MeV seems to be strongly suppressed in this case. To go down in the beam energy might be a possibility to trace such a contribution because of stronger CC effects. For example, our folding model analysis of the elastic and inelastic $\alpha+^{12}$C data at $E_\alpha = 104$ MeV [37, 38] has shown that the CC effects substantially increase the ratio $\sigma_{2_2^+}/\sigma_{3_1^-}$ (from 12.6% in the DWBA

up to about 27% in the CC results). However, no angular distribution has been measured for the 3_1^- state at this energy and it is, therefore, difficult to make a similar discuss about the 2_2^+ state.
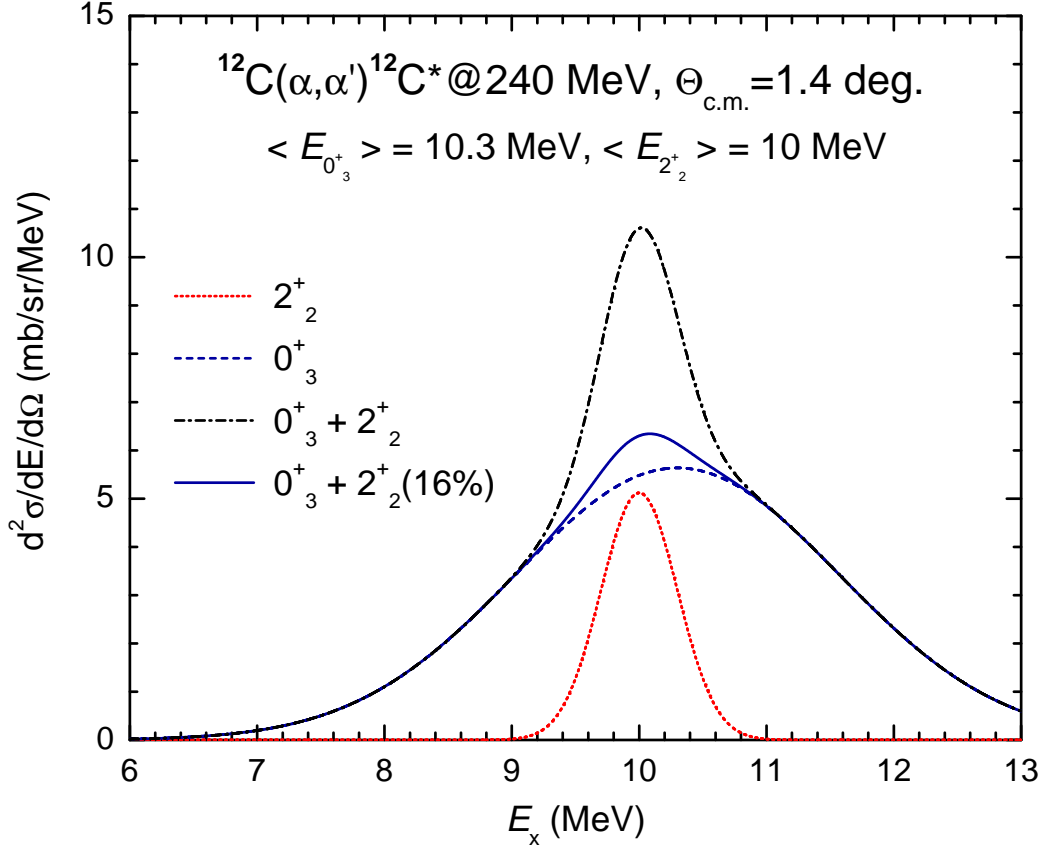

Figure 4: Decomposition of the 240 MeV $(\alpha, \alpha')^{12}$C cross sections at $\Theta_{c.m.} = 1.4°$, predicted in the DWBA for the 0_3^+ and 2_2^+ states, into the Gaussians of 3 MeV and 0.6 MeV widths, respectively. See more details in text.

Situation becomes more complicated when we move up by about 500 keV in the excitation energy to the 0_3^+ peak at $E_x \approx 10.3$ MeV. The predicted

ratio of integrated cross sections is $\sigma_{2_2^+}/\sigma_{0_3^+} \approx 81\%$ in the DWBA calculation of $(\alpha,\alpha')^{12}$C scattering at 240 MeV. Therefore, if the 2_2^+ state is located around 10 MeV, the $(\alpha,\alpha')^{12}$C cross section for the 2_2^+ state should strongly interfere with that of the 0_3^+ state but such an effect has not been reported experimentally [12]. To investigate this effect we have made an *inverse* multipole decomposition analysis by spreading the inelastic $\alpha+^{12}$C scattering cross sections at $\Theta_{\text{c.m.}} = 1.4°$, predicted in the DWBA for the 0_3^+ and 2_2^+ states, into the Gaussians of 3 MeV and 0.6 MeV widths, respectively, as deduced for the 0_3^+ peak from the $(\alpha,\alpha')^{12}$C spectrum at $E_\alpha = 240$ MeV [12] and for the possible 2_2^+ peak from the $(p,p')^{12}$C spectrum at $E_p = 66$ MeV [17]. The results of this decomposition analysis are plotted in Fig. 4 where the area of each Gaussian has been normalized to the predicted DWBA cross section and the centroids of the 0_3^+ and 2_2^+ peaks assumed to be around 10.3 and 10 MeV, respectively. Given no strong interference between the 0_3^+ and 2_2^+ angular distributions observed in the 240 MeV experiment, we have tried to trace the remnant of the 2_2^+ state by reducing its strength in such a way that the centroid of the sum of two Gaussians $(0_3^+ + 2_2^+)$ remains within the experimental value of 10.3 ± 0.3 MeV as deduced from the 240 MeV data [12] for the 0_3^+ peak. Namely, by reducing the 2_2^+ cross section to around 16% of its predicted strength at $\Theta_{\text{c.m.}} = 1.4°$, we obtained the sum of the two $(0_3^+ + 2_2^+)$ Gaussians centered at $E_{\text{x}} \approx 10.2$ MeV (see solid curve in Fig. 4). To further trace such a remnant of the 2_2^+ state in the $(\alpha,\alpha')^{12}$C cross section at 240 MeV we have made the DWBA calculation using the inelastic FF's given by the full AMD transition densities for the 0_3^+ and 2_2^+ states as well as the FF given by the AMD transition density for the 2_2^+ state scaled
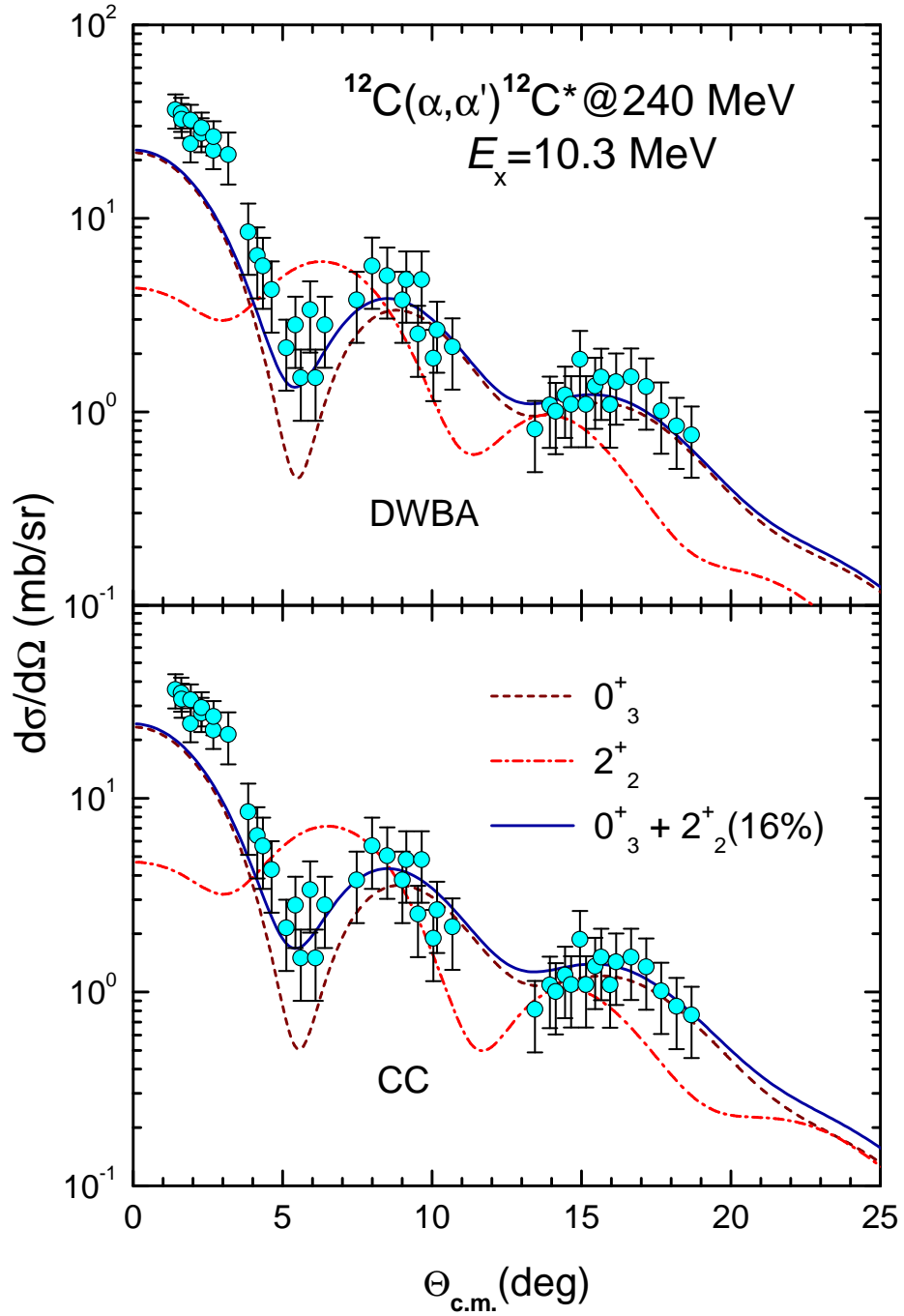
17

Figure 5: Inelastic $\alpha + {}^{12}C$ scattering data measured for the 0_3^+ state at $E_x \approx 10.3$ MeV [12] in comparison with the DWBA and CC cross sections given by the complex double-folded inelastic FF based on the AMD nuclear transition densities for 0_3^+ and 2_2^+ states. The total cross section (solid curve) contains only 16% of the predicted 2_2^+ cross section.

18

by a factor of 0.4 that corresponds to the 16% reduction of the 2_2^+ cross section. From the comparison of these DWBA results with the measured angular distribution for 0_3^+ state in upper panel of Fig. 5 one can see that the AMD transition density for the 0_3^+ state describes the data quite reasonably and, hence, the monopole transition moment $M(E0)$ given by the AMD (see Table 1) should be close to the realistic value. Although rather small, the 16% contribution of the 2_2^+ cross section helps to significantly improve the agreement with the data at the diffractive minimum around $\Theta_{\text{c.m.}} = 6°$. The scaling of the AMD transition density for the $0_1^+ \to 2_2^+$ excitation by a factor of 0.4 shows the measure of suppression of the 2_2^+ state in this case. If we apply the same scaling to the mixture of the 2_2^+ state in the spectrum of the 3_1^- state then the ratio $\sigma_{2_2^+}/\sigma_{3_1^-} \approx 2.4\%$ that is too small to be extracted from the measured spectrum for the peak around 9.6 MeV. Independently, such a conclusion can be well drawn from the measured data shown in Fig. 2. Therefore, it is reasonable to assume in the CC calculation of the $(\alpha, \alpha')^{12}$C cross sections for the 0_3^+ and 2_2^+ states at $E_{\text{x}} \approx 10$ MeV the same scaling for all inelastic FF corresponding to the transitions to and from the 2_2^+ state shown in Fig. 3. The CC results obtained with the scaled inelastic FF are shown in lower panel of Fig. 5. We found that the coupling effects enhance the 2_2^+ cross section by about 50%, with a slight change of the 0_3^+ cross section, and that leads to a much better agreement with the data points over the whole angular region. The improved agreement with the data points by the CC results indirectly indicate that the contribution from the 2_2^+ state is not negligible as in the case of the 3_1^- state and it smoothens the measured 0_3^+ angular distribution at 240 MeV as shown in Fig. 5. In other words,

about 40% of the predicted strength of the AMD wave function $\Psi_{2_2^+}$ could be hidden in $(\alpha, \alpha')^{12}$C spectrum measured at 240 MeV for the 0_3^+ state. The AMD calculation has shown that the 0_3^+ and 2_2^+ states have quite similar extended cluster structures (see Fig. 5 of Ref. [11]) and are almost degenerate at $10.6 \sim 10.7$ MeV. The most striking is a very strong "interband" transition $B(E2, 0_3^+ \rightarrow 2_2^+) \approx 1553 \ e^2\text{fm}^4$, predicted by the AMD, which helps to enhance the 2_2^+ cross section by about 50% in the CC calculation. Thus, we have found that a *ghost* of the 2_2^+ state seems to be present in the measured 0_3^+ angular distribution and following conclusions can be drawn from our CC analysis of the 240 MeV $(\alpha, \alpha')^{12}$C data:

- If the 2_2^+ state is located at the peak observed at $E_x \approx 11.46$ MeV then its width should be large enough to allow a tail of this peak to overlap with the broad 0_3^+ peak. A direct CC analysis of the $(\alpha, \alpha')^{12}$C cross section measured for the energy bin centered at 11.46 MeV using the AMD wave function might solve this issue but no experimental angular distribution is available for that purpose.

- If the 2_2^+ state is located at $E_x \approx 9 \sim 10$ MeV, as predicted by some cluster calculations, then it should be hindered by the strong 3_1^- peak and only a weak fraction of its strength (about 16%) is mixed with the broad 0_3^+ peak.

The measured angular distribution has been subjected to a multipole decomposition analysis to disentangle contribution of different multipolarities $(\lambda = 0, 1, 2, 3)$ to the excitation of ^{12}C in each energy bin, in the same way as done, e.g., in the inelastic α-scattering study of IS giant resonances in
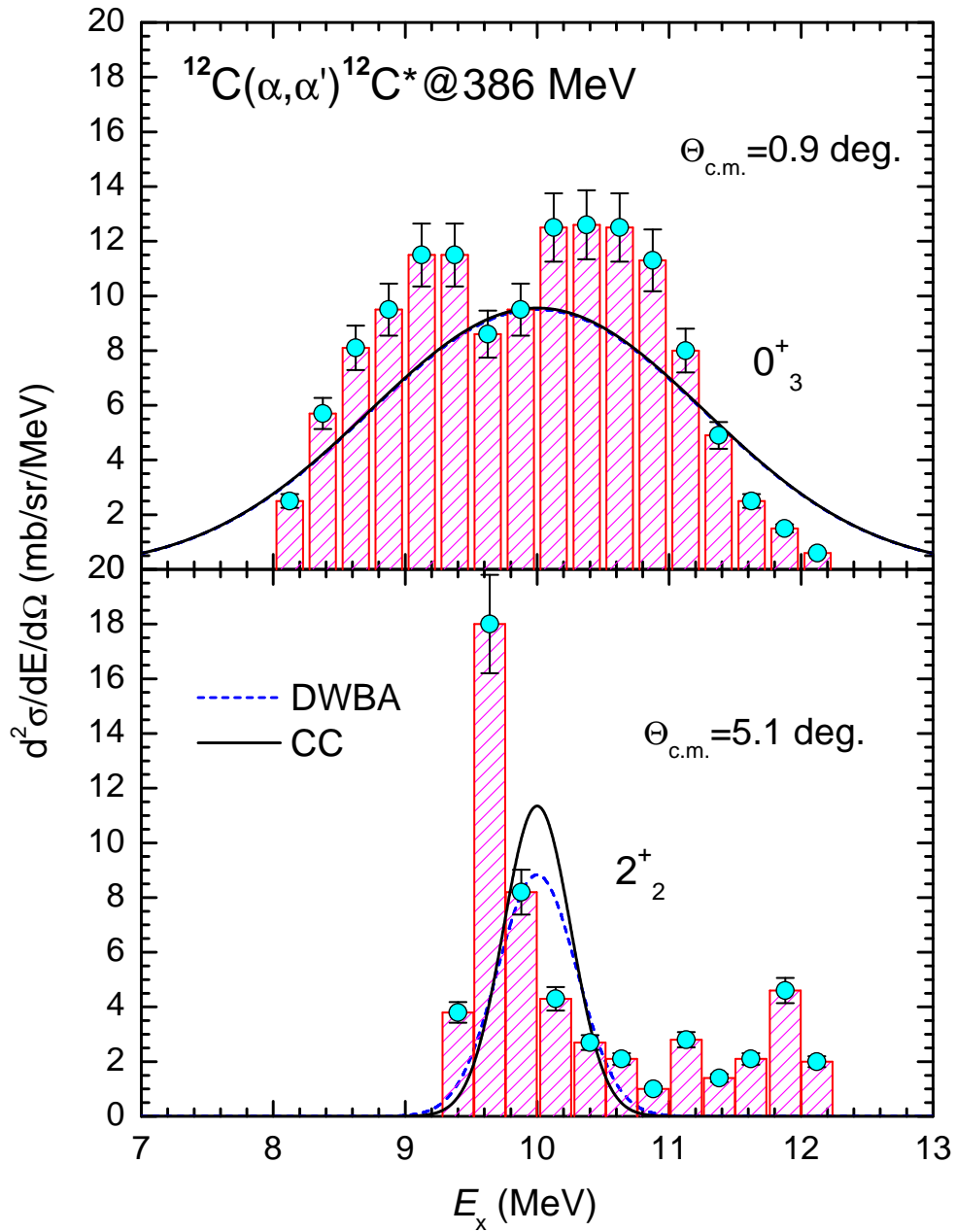
Figure 6: The same decomposition as in Fig. 4 but for the 386 MeV $(\alpha, \alpha')^{12}$C cross sections at $\Theta_{c.m.} = 0.9$ and $5.1°$ predicted in the DWBA and CC formalism in comparison with the measured data taken from Ref. [13]. See more details in text.

^{208}Pb [39]. It is, therefore, possible to compare the predicted AMD transition strengths for the 0_3^+ and 2_2^+ state with the experimental spectrum at some particular scattering angle. For this purpose, we have done similar decomposition of the 386 MeV $(\alpha, \alpha')^{12}$C cross sections at $\Theta_{\text{c.m.}} = 0.9°$ and $5.1°$, predicted in the DWBA and CC formalism for the 0_3^+ and 2_2^+ states, respectively, and the results are plotted in Fig. 6 together with the corresponding double differential cross section measured at $E_\alpha = 386$ MeV [13]. As can be seen in upper panel of Fig. 6, the AMD transition density for the 0_3^+ state accounts fairly well for the data points measured at the forward angle, with the integrated cross section (over the excitation energy) $d\sigma/d\Omega \approx 30$ mb/sr compared to the experimental value of around 33 ± 3 mb/sr. Contrary to the situation for the 2_2^+ state in the 240 MeV case, the full transition strength predicted by the AMD still significantly underestimates the observed strength (see lower panel of Fig. 6), with the DWBA integrated cross section $d\sigma/d\Omega \approx 6.6$ mb/sr at $\Theta_{\text{c.m.}} = 5.1°$ compared to the experimental value of around 13 ± 2 mb/sr. It becomes obvious now that in the case of the 2_2^+ state of ^{12}C one has to deal with about the same experimental difficulty as that in a study of isoscalar giant resonances, in disentangling different IS excitation modes when their energies overlap. In this sense, it is of interest to apply our AMD + folding approach to the inelastic $\alpha+^{12}$C scattering data measured at $E_\alpha = 386$ MeV by Itoh et $al.$ [13, 14]. We note that these authors were able to measure the $(\alpha, \alpha')^{12}$C energy spectrum without contamination from the instrumental background by using the high-resolution magnetic spectrometer Grand Raiden, and the $(\alpha, \alpha')^{12}$C angular distribution has been deduced for each 250 keV energy bin in the excitation energy range $3 \lesssim E_{\text{x}} \lesssim 20$ MeV
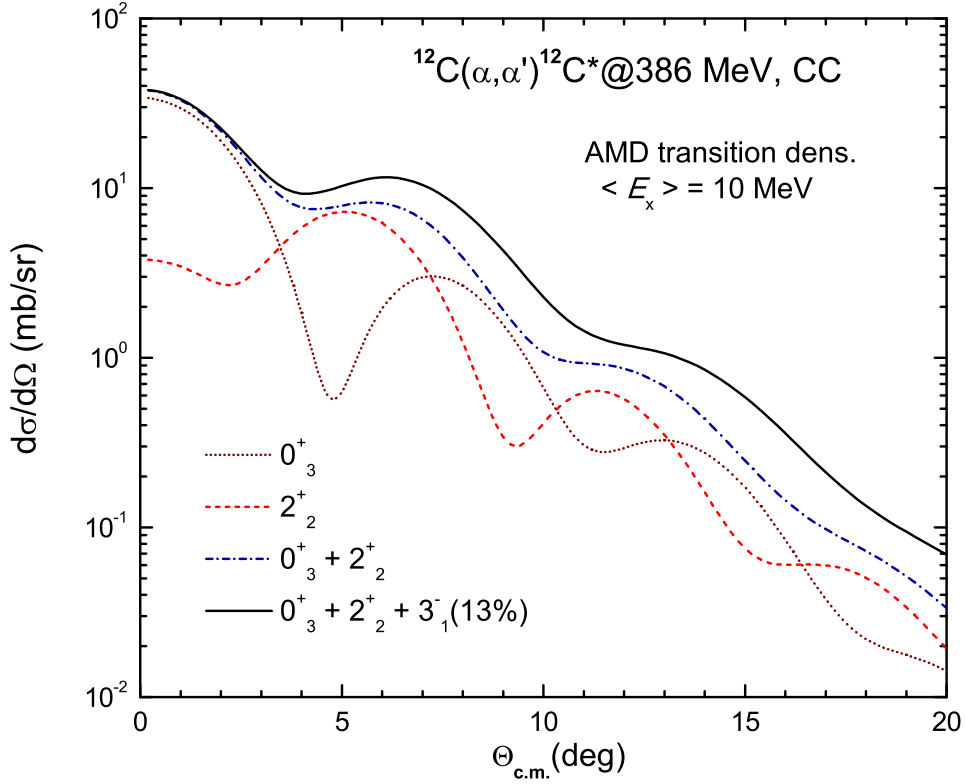
Figure 7: The CC results for the $(\alpha, \alpha')^{12}$C cross section at 386 MeV obtained with the AMD transition densities. The total cross section (solid curve) contains a 13% contamination from the 3_1^- state and agrees well with the experimental angular distribution deduced for the excitation energy $\langle E_x \rangle \approx 10$ MeV [14]. See more details in text.

[13, 14].

The CC calculation enhances the integrated cross section to $d\sigma/d\Omega \approx 7.3$ mb/sr that is still well below the experimental value. Because the strongest peak in the experimental spectrum of the 2_2^+ state is located at $E_x \approx 9.6$ MeV, in about the same position as that of the 3_1^- state, it is not excluded that this experimental spectrum has some contamination from the transition strength of the 3_1^- state [40]. Moreover, as shown in our recent folding model analysis of inelastic $\alpha + ^{208}$Pb scattering to the IS giant resonances in ^{208}Pb,

23

the IS transition strengths for a given 2^λ-pole excitation given by the MDA of the data measured at 240 MeV [41] and 386 MeV [39] could be slightly different due to possible contribution from the pickup/breakup reaction as well as different maximum λ values taken into account in the MDA. Keeping in mind possible uncertainty of the MDA, we have made an estimation of the 3_1^- contamination in the experimental spectrum measured at 386 MeV for the 2_2^+ state, based on the IS transition strengths predicted by the AMD [11]. To achieve a visually good agreement of our CC results with the preliminary data measured at 386 MeV for the total $0_3^+ + 2_2^+$ cross section summed over the energy bins around $E_x = 10$ MeV [14], we need to add to the predicted $0_3^+ + 2_2^+$ cross section a significant contribution from the 3_1^- cross section. These CC results are shown in Fig. 7 and one can see that the contamination by the 3_1^- cross section in the measured angular distribution could be up to 13% or more. Therefore, we conclude that at least 36% of the predicted strength of the wave function $\Psi_{3_1^-}$ could be hidden in the measured 386 MeV $(\alpha, \alpha')^{12}$C cross section shown in Fig. 2 of Ref. [14]. Such a mixture of the 3_1^- state could also affect the angular correlation function of the α-decay from the excited ^{12}C* nucleus at $E_x \approx 10$ MeV (see Fig. 3 in Ref. [14]). Nevertheless, the fact that the full (direct and indirect) transition strengths predicted for the 2_2^+ state still underestimate the measured $(\alpha, \alpha')^{12}$C spectrum (see Fig. 6) and angular distribution (see Fig. 7) indicates that the authors of Refs. [13, 14] were able to extract the full $E2$ transition strength of the 2_2^+ state from the 386 MeV $(\alpha, \alpha')^{12}$C spectrum, even though the 2_2^+ peak is located right behind the strong 3_1^- peak.

In conclusion, a detailed folding model analysis of the $(\alpha, \alpha')^{12}$C data at

240 and 386 MeV in the DWBA and CC formalism has been performed, using the nuclear transition densities predicted by the AMD approach and a complex CDM3Y6 interaction. From the structure point of view, given a very weak transition rate $B(E2; 0_1^+ \to 2_2^+)$ predicted by the AMD, the direct excitation of the 2_2^+ state should be an unlikely event in any reaction and that could be the reason why it was so difficult to identify the 2_2^+ state in the excitation energy- and/or α-decay spectra of ^{12}C. Nevertheless, we have shown here some evidence for a *ghost* of the 2_2^+ state in the 240 MeV $(\alpha, \alpha')^{12}$C angular distribution measured at $E_x \approx 10.3$ MeV, which should be a tail of the 2_2^+ peak located either at 11.46 MeV or right behind the 3_1^- peak at 9.64 MeV. In addition to the weak transition $0_1^+ \to 2_2^+$, the strong 3_1^- peak was shown to be the main hindrance for the experimental identification of the 2_2^+ state.

The AMD transition densities account reasonably for the relative contributions from the 2_2^+ and 0_3^+ states to the 386 MeV $(\alpha, \alpha')^{12}$C angular distribution measured at $\langle E_x \rangle \approx 10$ MeV. We also found a contamination of about 13% from the 3_1^- state in this angular distribution. Although the 2_2^+ state was found to be located near the strong 3_1^- peak, its full $E2$ strength has been carefully deduced from the 386 MeV $(\alpha, \alpha')^{12}$C spectrum and these data [13, 14] remain so far the only experimental evidence of the 2_2^+ state at $E_x \approx 10$ MeV.

Finally, going down in the beam energy might be an alternative to search for the 2_2^+ peak in the $(\alpha, \alpha')^{12}$C measurement because of very strong indirect transition $0_2^+ \to 2_2^+$ that can be induced as a two-step excitation of the 2_2^+ state in the CC scheme. However, before discussing the indirect excitation

of the 2_2^+ state, we must check which reaction channel is more likely for the Hoyle state: the direct α-decay or isoscalar $E2$ excitation. That should be an interesting perspective for a future study of inelastic $\alpha+^{12}C$ reaction within the coupled reaction channel formalism.

References

[1] M. Freer, Rep. Prog. Phys. 70 (2007) 2149.

[2] Y. Funaki, H. Horiuchi, W. von Oertzen, G. Röpke, P. Schuck, A. Tohsaki, T. Yamada, Phys. Rev. C 80 (2009) 064326.

[3] E. Uegaki, S. Okabe, Y. Abe, H. Tanaka, Prog. Theor. Phys. 57 (1977) 1262.

[4] M. Kamimura, Nucl. Phys. A 351 (1981) 456; M. Kamimura, private communication.

[5] R. Pichler, H. Oberhummer, A. Csoto, S.A. Moszkowski, Nucl. Phys. A 618 (1997) 55.

[6] A. Tohsaki, H. Horiuchi, P. Schuck, G. Röpke, Phys. Rev. Lett. 87 (2001) 192501.

[7] Y. Funaki, A. Tohsaki, H. Horiuchi, P. Schuck, G. Röpke, Phys. Rev. C 67 (2003) 051306(R).

[8] M. Chernykh, H. Feldmeier, T. Neff, P. von Neumann-Cosel, A. Richter, Phys. Rev. Lett. 98 (2007) 032501.

[9] Y. Funaki, A. Tohsaki, H. Horiuchi, P. Schuck, G. Röpke, Eur. Phys. J. A 24 (2005) 321.

[10] C. Kurokawa and K. Katō, Nucl. Phys. A 738 (2004) 455.

[11] Y. Kanada-En'yo, Prog. Theor. Phys. 117 (2007) 655.

[12] B. John, Y. Tokimoto, Y.W. Lui, H.L. Clark, X. Chen, D.H. Youngblood, Phys. Rev. C 68 (2003) 014305.

[13] M. Itoh *et al.*, Nucl. Phys. A 738 (2004) 268.

[14] M. Itoh *et al.*, Proc. of the 23rd Intern. Nucl. Phys. Conf. (INPC2007), Elsevier B.V., 2008, p.371.

[15] M. Freer *et al.*, Phys. Rev. C 76 (2007) 034320.

[16] C. Aa. Diget *et al.*, Phys. Rev. C 80 (2009) 034316.

[17] M. Freer *et al.*, Phys. Rev. C 80 (2009) 041303(R).

[18] T. Muñoz-Britton *et al.*, J. Phys. G 37 (2010) 10510.

[19] D.T. Khoa, D.C. Cuong, Phys. Lett. B 660 (2008) 331.

[20] D.T. Khoa, Intern. J. Modern Phys. E 17 (2008) 2055.

[21] D.T. Khoa, G.R. Satchler, Nucl. Phys. A 668 (2000) 3.

[22] D.C. Cuong, D.T. Khoa, G. Colò, Nucl. Phys. A 836 (2010) 11.

[23] Y. Kanada-En'yo, H. Horiuchi, A. Ono, Phys. Rev. C 52 (1995) 628;
     Y. Kanada-En'yo, H. Horiuchi, Phys. Rev. C 52 (1995) 647.

[24] M.N. Harakeh, A.E.L. Dieperink, Phys. Rev. C 23 (1981) 2329;
     N.V. Giai, H. Sagawa, Nucl. Phys. A 371 (1981) 1.

[25] T. Neff, private communication on the FMD results (unpublished).

[26] F. Ajenberg-Selove, Nucl. Phys. A 433 (1985) 1.

[27] G.M. Reynolds, D.E. Rundquist, R.M. Poichar, Phys. Rev. C 3 (1971)
     442.

[28] S. Raman, C.W. Nestor Jr., P. Tikkanen, At. Data and Nucl. Data
     Tables 78 (2001) 1.

[29] P. Strehl, Z. Phys. 234 (1970) 416.

[30] P.M. Endt, At. Data and Nucl. Data Tables 23 (1979) 3; F. Ajenberg-
     Selove, Nucl. Phys. A 506 (1990) 1.

[31] T. Kibedi, R.H. Spear, At. Data and Nucl. Data Tables 80 (2002) 35.

[32] D.T. Khoa, G.R. Satchler, W. von Oertzen, Phys. Rev. C 56 (1997) 954.

[33] D.T. Khoa, Phys. Rev. C 63 (2001) 034007.

[34] J. Raynal, in *Computing as a Language of Physics* (IAEA, Vienna, 1972) p.75; J. Raynal, coupled-channel code ECIS97 (unpublished).

[35] D.T. Khoa, W. von Oertzen, H.G. Bohlen, S. Ohkubo, J. Phys. G 34 (2007) R111.

[36] G.R. Satchler, D.T. Khoa, Phys. Rev. C 55 (1997) 285.

[37] G. Hauser, R. Löhken, H. Rebel, G. Schatz, G.W. Schweimer, J. Specht, Nucl. Phys. A 128 (1969) 81.

[38] J. Specht, G.W. Schweimer, H. Rebel, G. Schatz, R. Löhken, G. Hauser, Nucl. Phys. A 171 (1971) 65.

[39] M. Uchida *et al.*, Phys. Rev. C 69 (2004) 051301(R).

[40] M. Itoh, private communication (unpublished).

[41] D.H. Youngblood, Y.W. Lui, H.L. Clark, B. John, Y. Tokimoto, X. Chen, Phys. Rev. C 69 (2004) 034315.